IBIS/PICsIT Instrument Specific Software Scientific Validation Report

L. Foschini, V. Bianchin, A. Goldwurm, A. Gros, G. Malaguti, P. Laurent, L. Natalucci

Approved by P. Ubertini (IBIS PI), G. Di Cocco (IBIS CoPI)

Version 6.0

RI IASF n. 491
April 6, 2007

	Revision History
v 1.0	First version for first software release of March 2003.
28/02/2003	
v 1.1	Update for the intermediate software release of May 2003.
30/04/2003	Early analysis of Cyg X–1, cleaning of cosmic–ray induced events,
	improvement of the position accuracy, comparison with ECOE data.
v 1.2	Update for OSA 3 release.
27/10/2003	Crab in rev 102; automatic source location; timing analysis.
	Some error corrected. Removed the non–standard analysis section.
v 2.0	General reshape of the document style. Update for OSA 3.1 release.
02/02/2004	Updated the discussion on the uniformity maps and the inclusion of GTI.
v 4.0	Update for OSA 4 release (jump in the version number to match the OSA version).
06/07/2004	New executable for mosaic. New background maps.
v 5.0	Update for OSA 5 release. Revision of deconvolution algorithm.
28/07/2005	Module for spectra extraction.
v 5.1	Update for OSA 5.1 release.
07/12/2005	Background studies.
v 6.0	Update for OSA 6.0 release.
06/04/2007	Update of RMF/ARF and the instrument monitoring.

1 Introduction

This report summarizes the scientific performances and reliability of the Instrument Specific Software (ISSW) of the PICsIT detector layer of the IBIS imager aboard INTEGRAL (see Di Cocco et al. 2003 for more details on the instrument). The executables analysed here, together with their Instrument Configuration (IC) files, are those delivered by the IBIS Team to the ISDC for the integration in the Off–line Scientific Analysis (OSA) software package version 5.1 released by the ISDC to the public by 24 November 2005. An equivalent report on the IBIS/ISGRI ISSW is provided in a separate document by A. Goldwurm et al. (IBIS/ISGRI Instrument Specific Software Scientific Validation Report).

The basic concepts of the scientific analysis of the IBIS telescope are described in Goldwurm et al. (2001, 2003), while more detailed technical information about the pipelines, data structures, tools, and complementary modules can be found in the documents *Introduction to INTEGRAL Data Analysis* (ISDC/OSA–INTRO), *ISDC Data Repository Organization* (ISDC/TEC013), and *IBIS Analysis User Manual* (ISDC/OSA–UM–IBIS). Specific descriptions, performances, and problems of the pipeline scripts or other executables not provided by the IBIS Instrument Team (IT), as well as installation problems, operating systems compatibility, hardware load, and so on, are not analyzed and reported here.

This report provides a evaluation of the scientific performances of the IBIS/PICsIT software according to the tests performed so far. Further tests will be available in the next versions of the present document. We also underline that this document does not provide a comprehensive analysis and evaluation of the IBIS/PICsIT in-flight calibrations and instrument performances, although some results described in the present report can be used for that purpose.

2 The IBIS/PICsIT data analysis

2.1 General concepts

The general purpose in the data analysis of astronomical instruments can be basically divided into two parts: the first, based on the analysis of images, is to measure the celestial coordinates, the spatial structure (extended or point–like sources), and the photometry of the source. The second, related to the study of the spectra, is to measure the flux and energy of emission/absorption lines, and the characteristics of the continuum. The measuring process adds several effects that contribute to modify the original image or spectrum. Therefore, it is necessary to operate corrections to the data in order to obtain an image/spectrum that is as much as possible consistent with the original one. Despite the differences depending on the instrument used in the observation, from a purely conceptual point of view, it is necessary to solve an inverse problem with distribution functions. In other words, by assuming for the sake of simplicity a monodimensional case, we have to solve the following integral equation of Fredholm of the first kind:

$$\phi(x) = \int \psi(z) K(x,z) dz \tag{1}$$

where ϕ is the observed density of probability function, while ψ is the corresponding original density of probability fuction that we want to restore. K is the kernel of the integral equation and represents the measuring process, including the effects of the measuring errors in the observed distribution. The kernel is called *point–spread function* (PSF) in the images, while it is called *line–spread function* (LSF) in the spectra. ϕ, ψ, and K are all non–negative functions, since they are connected with the density of the incoming photons.

The basic problem of the astronomical software is therefore "to clean" the PSF or LSF from all the systematic errors (including those of calibrations), before to proceed to the inversion of the integral equation. At the end of the correction ("cleaning") process, the kernel should contain only the statistical errors intrinsic to the measuring process. For example, in the case of a gaussian distribution with variance σ^2, the kernel is:

$$K(x,z) = \frac{1}{\sigma\sqrt{2\pi}} \exp \frac{-(x-z)^2}{2\sigma^2} \tag{2}$$

Depending on the type of instrument, there are different types of corrections. A system for astronomical data processing can be divided into three main steps, which in turn can be divided into sub–steps. The first step (**Level 0**) is the *preprocessing* level, where the telemetry coming from the satellite is unpacked and converted into a standard format (FITS) (see in the ISDC Technical Document section[1]). The basic data structure (RAW and PRP) is built, together with the On–Board Time (OBT) information, and the division into Science Windows (ScW) is set up (see ISDC/TEC013 for more details).

It is worth noting that, in the case of IBIS/PICsIT, there is also an on–board processing of the data before the Level 0, performed by the Hardware Event Preprocessor of IBIS (HEPI). This is necessary because of the limited telemetry available on–board the INTEGRAL satellite and the high count rate of background (≈ 3500 c/s) in the IBIS/PICsIT energy range ($0.17 - 10$ MeV). Therefore, HEPI performs a preliminary processing of the event list (containing the position y, z of the pixel, the channels $0 - 1023$, and the time information), before to send it to the ground. The corrections are: equalization by applying the gain and offset values of the HEPI look–up tables (LUT), conversion from channels to energy to reconstruct the multiple events, integration of events into histograms to save telemetry. The histograms are divided into two types: one (*spectral imaging*) is a data cube of $256 \times 64 \times 64$, containing still the full spatial information (64×64 pixel) and a moderate energy resolution (from the original 1024 to 256 channels). The integration time of a single histogram is generally corresponding to the duration of one ScW (≈ 2000 s), resulting in a loss of time information. Therefore, to perform time study, the other type of histogram (*spectral timing*) is designed to keep time resolution down to 1 ms, but with a great loss of energy resolution (from 1024 to 8 channels), and without spatial information. The combination of the *spectral imaging* and *spectral timing* is called *standard mode*. It is worth noting that IBIS/PICsIT can download directly the event list, without the integration on–board (*photon–by–photon* mode PPM), but with great consumption of telemetry. Therefore, with the exception of some observations of calibration, IBIS/PICsIT works only in standard mode, by producing spectral imaging histograms for single and multiple events, and histograms in spectral timing (default 4 energy bands and 4 ms of time resolution). More details on IBIS/PICsIT on–board processing are available in the IBIS User Manual, Issue 5.1.

Once the basic data structure is set up, there is the correction step (**Level 1**) where the instrument dependent corrections are applied. In this level, the OSA pipeline starts to work and perform the sublevels COR, DEAD, GTI, BIN_I/BIN_S, BKG_I/BKG_S. The specific corrections for IBIS/PICsIT are:

1. the intrinsic deadtime of the detector, that is the time during which it is not possible to process any event, since the detector is devoted to the processing of another event;
2. additional deviations from the on–board tables of gain and offset (only for PPM), and conversion from channels to energy;
3. filtering of the events according to the Good Time Intervals (GTI); for PPM only;
4. correction of partially downloaded histograms (for standard mode only);
5. correction for detector non–uniformities and subtraction of the background.

[1] Available at `http://isdc.unige.ch/index.cgi?Documents+doctec`.

When the data are cleaned from background and corrected for instrumental effects, it is possible to move to the third level (**Level 2**), where the creation of images, spectra, and lightcurves is done (sublevels CAT_I/CAT_S, IMA/IMA2, SPE, LCR). The shadowgrams, produced in the previous level, are deconvolved according to the algorithms explained in Goldwurm et al. (2001, 2003), and the search for known sources is done, starting from a general catalog (Ebisawa et al. 2003). The attitude values of right ascension and declination obtained from the star tracker are referred to IBIS/PICsIT, by using a rotation and traslation (IBIS/PICsIT and the star tracker are not aligned). Moreover, the deconvolved image is projected into the sky with the gnomonic projection (TAN, cf Calabretta & Greisen 2002). The standard products of the source detection, performed on the sky images, is composed of the source coordinates and errors (in celestial coordinates and in pixels), the flux and its error (in counts per second), and the significance.

In the part of the extraction of the spectra, whose algorithms are still described in the seminal papers by Goldwurm et al. (2001, 2003), two IC files are of extreme importance. The first, named Auxiliary (or Ancillary) Response File (ARF) contains the information about the effective area of the detector as a function of the photon energy. The second IC file is named Redistribution Matrix File (RMF) and contains the information necessary to convert the counts into photons. A full description of the IBIS RMF/ARF is presented in Laurent et al. (2003).

The lightcurves are generated by using the spectral timing data, and therefore they are simply the count rates versus time for the whole detector. The deadtime and barycentric corrections are applied. The extraction of lightcurves for single point sources is not yet implemented, since it can be done only in PPM.

The output of the OSA pipeline can be analysed by means of the common software for high–energy astrophysics (e.g. `xspec`, `ds9`, `xronos`, ...).

2.2 General description of the executables

The IBIS/PICsIT–ISSW delivered to date for the Scientific Analysis of the PICsIT data include:

- `ibis_pics_deadtime` (v 2.4.1, 31 May 2004, DEAD level):
  to calculate the intrinsic deadtime of each semimodule of the detector. It is based on the use of a specific IBIS/PICsIT housekeeping, the *livetime counter*, that provides already the effective live time for each semimodule every 8 seconds. It provides also a display for the temperatures of each module.
- `ip_ev_correction` (v 1.8, 6 September 2005, COR level):
  to perform a correction of gain and offset variations in addition to those performed on board by HEPI. It is only for data obtained in photon–by–photon mode. It is strictly linked with the IC data structure `PICS-ENER-MOD`, containing the average gain, offset, and the deviations, pixel by pixel, from these values. Presently, no deviations are implemented, that is, only the onboard equalization are used. See Malaguti et al. (2003) for details on in-flight gain/offset behaviour.
- `ip_ev_shadow_build` (v 2.7, 27 June 2006, BIN_I/BIN_S level):
  to perform the building of the shadowgrams and the efficiency maps (dimensions 64×64) from data in photon–by–photon mode, according to energy bands or time bins selected by the user. The events are cleaned from the spurious events induced by cosmic-rays or noisy pixels (see Sect. 5 for more details) and selected according to the available table of Good Time Intervals (GTI), which in turn are generated by another set of executables made by ISDC.
- `ip_si_shadow_build` (v 3.2, 26 June 2006, BIN_I/BIN_S level):
  to perform the building of shadowgrams and the efficiency maps (dimensions 64×64) from

the dat in standard mode (spectral imaging). It reads the binning tables from the IC file PICS-BINT-CFG (containing the data of the onboard HEPI LUT) and converts into channels the requested energy bands. By default, if histograms are not complete, the executable returns simply a warning, but it continues the analysis by discarding it. If the user wants to correct and use also partially downloaded histograms, it is possible to set the threshold below which the executable correct (the missing pixels will be trated as killed pixels) and integrate the partially downloaded histograms. The parameter to set is IBIS_IPS_corrPDH, that has to be put equal to the maximum number of allowed missing cells. It is better to keep IBIS_IPS_corrPDH$\leq$ 10000. In rev_2 data type, it is possible to discard also those shadowgrams affected by problems in resynchronization of HEPI (see IA19 and SCREW1406).

- ip_shadow_ubc (v 3.1, 24 March 2004, BKG_I/BKG_S level):
  to perform the correction for background and detector non–uniformities. The output shadowgrams are also expanded to take into account the gaps between modules (from 64×64 to 65×67). The gaps and the killed pixels are filled with a mean value of counts averaged over the whole detector. There is also a variance map, calculated starting from the statistical variance of the detector counts and updated according to the correction performed (filled pixels, background subtraction, and so on...). The executable is linked with the following IC data structures: PICS-SBAC-BKG (background maps for single events), PICS-MBAC-BKG (background maps for multiple events), PICS-SUNI-BKG (detector non–uniformities for single events), and PICS-MUNI-BKG (detector non–uniformities for multiple events). See Sect. 3 and 4 for details.

- ip_skyimage (v 3.3, 29 June 2006, IMA2 level):
  it performs the deconvolution and sky image reconstruction by means of the algorithm described by Goldwurm et al. (2003). The executable provides a basic deconvolved sky image, significance, and variance maps. The latter are optional and the default is no variance maps in output (PICSIT_outVarian=0). The sky projection adopted is the gnomonic one (TAN[2]). It is also possible to use as input a set of variance shadowgrams already corrected for the background subtraction: in this case, the significances in output should be read as values already corrected for the background. This was the default option with previous releases of OSA: starting from OSA5, the default option will be to use the variance shadowgram not corrected, but there is the opportunity to return to the old way by setting the parameter PICSIT_inCorVar=1. For staring observation, it is possible to integrate the shadowgrams before the deconvolution and the automatic source location. For observations with dithering pattern, it is not possible to sum the shadowgrams before the deconvolution. Therefore, this module perform the basic deconvolution for every ScW. The weighted integration of the ScW images (mosaic) is the task of next executable. In this version, a global correction for off-axis effects (PSF distortion, SPIBIS effect[3], etc...). In order to disentangle the different contributions to the off-axis effects and to correct them separately more detailed studies are ongoing. Further developments are foreseen in future deliveries.

- ip_skymosaic (v 1.7, 16 November 2005, CLEAN level):
  it performs the integration of the individual ScW images into a single image (mosaic). It works mainly for dithering observations, but it can be used for staring pointings as well. It performs an integration with linear interpolation of the pixels, weight with the significance, and automatic source detection. The default sky projection is the gnomonic one (TAN), but it is possible also to change to stereographic (STG) or zenithal equidistant (ARC), the latter useful for polar regions. It is worth noting that PICsIT data work fine also with the varmosaic tool by K. Ebisawa provided by HEASoft v. 6.0: in this case, it is necessary that the OSA produce sky images per Scw with variance maps (i.e., set PICSIT_outVarian=1).

- ip_st_lc_extract (v 2.4, 3 March 2005, LCR level):
  it performs the extraction of the lightcurve of the whole detector from the spectral timing data. In the case of overflow error, the lightcurve is truncated to the latest useful value and

[2]For more information of sky projections, see Calabretta & Greisen (2002).
[3]See Barlow E.J., Bird A.J., Clark D.J., Dean A.J., Willis D.R.: Report on the SPIBIS study. August 2004.

an error message is written in the log file. The barycentric correction is not applied, and the output should be processed with the OSA tool `barycent`.

- `ip_spectra_extract` (v 2.2, 12 September 2005, SPE level):
  it performs the extraction of the spectrum of point sources from data in any mode (both photon-by-photon and standard), by using the Pixel Illumination Factor (PIF). Given the few sources detected (and expected) in the PICsIT energy range, the executable works for one single source. In this way, it is possible to make a simplified version of the algorithm described in Goldwurm et al. (2003). The energy bands are selected from the `RMF` file, that therefore should be rebinned according to the user's preferences before to run the pipeline.

It is worth noting that the OSA for IBIS/PICsIT makes use of other executables in addition to those described above (creation and merging of GTI, Catalog Extraction, and so on...). These executables have been developed by ISDC people (N. Produit, R. Rolhfs, L. Lerusse) and are not analysed here directly, although the proper working of these modules is essential to have the full software package. These executables work well to date.

3 Instrument monitoring and health

3.1 Background

IBIS/PICsIT operates in an energy region dominated by the background (that is also higher than expected from numerical models – cf Ferguson et al. 2003), where we expect that the source counts are of the order of a few percent of the global counts detected. This means that the background correction is of paramount importance for the instrument capabilities.

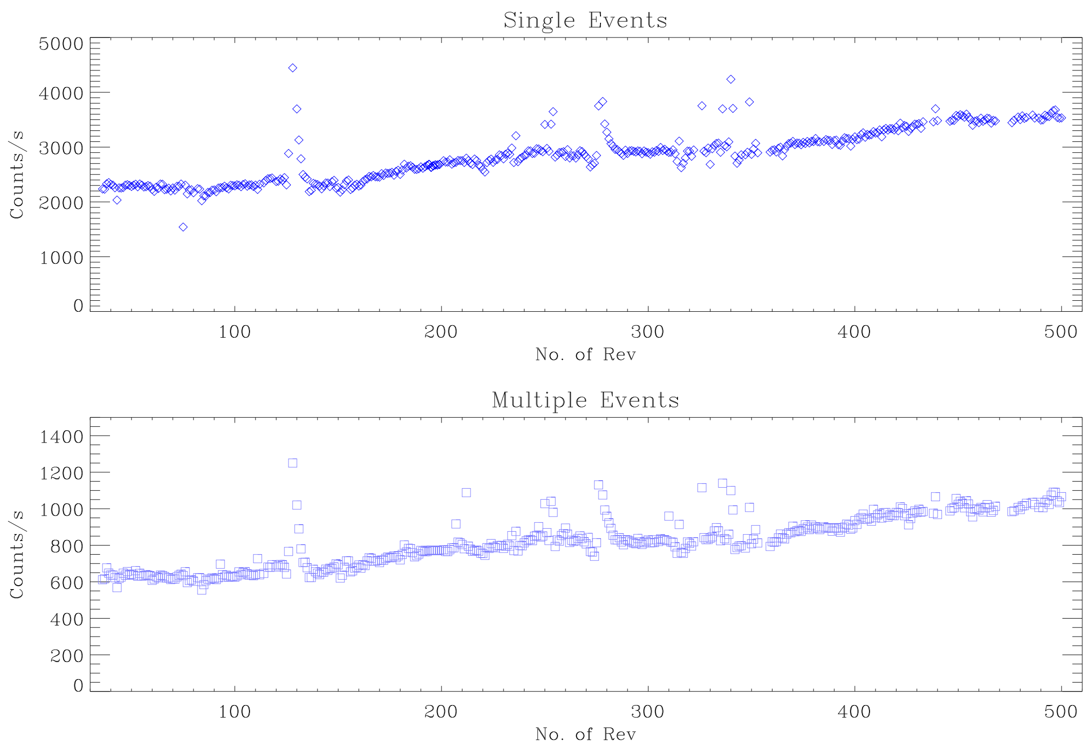

Figure 1: Background rates vs revolution number for single (*top panel*) and multiple events (*bottom panel*) in IBIS/PICsIT.

INTEGRAL was launched in 2002, just after the maximum of the Solar activity (occurred in 2000 − 2002), and therefore it was subject to increasing background fluxes, as shown in Fig. 1. A new Solar Cycle (n. 24) it is expected to start in 2007 – 2008 and this should reduce the background impacting on the instrument, although it is not yet known the impact of the activation of the detector. The instrument is kept under control in order to evaluate if in the forthcoming years an improvement of performances, due to decreasing background, can be expected.

3.2 Gain

The most important parameter to monitor the instrument health is the gain value, i.e. the energy width of each channel. In Fig. 2 it is displayed the gain behaviour versus the revolution number. The value remains almost stable around 7.0 − 7.1 keV/ch. As the revolution number increases, the error bar becomes larger and larger. This is likely to be due to the reductions of counts from the calibration source decay.

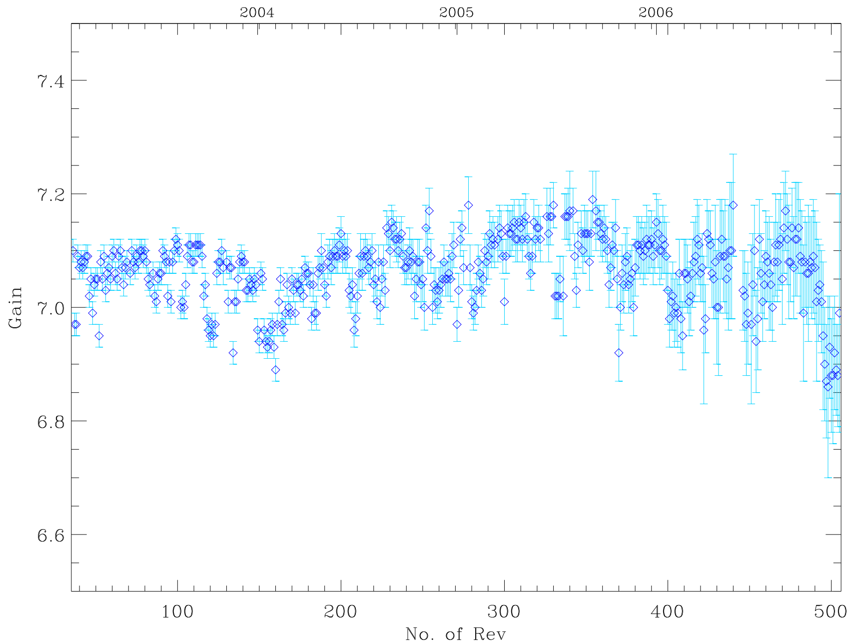

Figure 2: IBIS/PICsIT Gain values vs revolution number.

4 The correction for background in OSA

The photons interacting with IBIS/PICsIT are distributed in a non–uniform way, because of several reasons (see Natalucci et al. 2003 for more details). The main effect is to produce an enhancement of counts at the edges of the modules and semimodules. Therefore, before to perform the deconvolution, it is necessary to flatten the detector non-uniformities and to correct for the background. For this purpose, it is possible to use shadowgrams built from empty field observations, but it is also possible to integrate a long number of Scw also from pointed observations, because in the energy range of PICsIT ($0.2-10$ MeV) there are a few sources. Moreover, since *INTEGRAL* is operating mostly in dithering mode, this means that by summing all the shadowgrams pixel by pixel, any possible contribution of sources is blurred.

Major improvements in the background maps were already present in OSA4, with the availability of one set of maps with very long (1.7 Ms) exposures made by Piotr Lubinski (ISDC): these maps are stored in the files `pics_sbac_bkg_0007.fits` and `pics_mbac_bkg_0008.fits`. With OSA5, more background maps (still prepared by P. Lubinski), referring to different dates, are available (see Table 1), although the maps number 7 for singles and 8 for multiples should still be used as default.

These maps have been generated for a specific set of energy bands. This default set has been created to have the best source statistics, with the lowest possible contamination from background or other events, such as the cosmic–rays induced events (see Segreto et al. 2003), and the possibility to sum the maps of single and multiple events. These energy bands are shown in Table 2. It is worth noting that there was an update of the HEPI LUT during at the end of the revolution 169. The new binning table are slightly different from the previous one and led to some slight changes also in the energy bands (compare with Table 1 in the previous version of the present report). It is obvious that the user is free to select any type of energy band, but, in this case, he/she has also to built a new set of background maps.

Presently the executable contains two ways to rescale the background maps: according to the time of exposure and to the average value of counts. Although a more detailed study is necessary, it appears that the average value scaling could give better results.

Table 1: Set of background maps available with OSA5. Columns: (1) Start time of integrated data [YYYY-MM-DD]; (2) Number of map set (single/multiple events); (3) Exposures (single/multiple) [Ms]; (4) Revolutions integrated.

Date (1)	Single/Multiple (2)	Exposures (3)	Revs (4)
2003 – 03 – 09	0007/0008	1.7/1.4	49 – 67
2003 – 05 – 10	0008/0009	0.94/0.93	70 – 92
2003 – 08 – 02	0009/0010	0.38/0.38	97 – 103*
2003 – 09 – 24	0010/0011	1.4/1.4	115 – 123
2003 – 12 – 12	0011/0012	0.19/0.18	142 – 157
2004 – 02 – 07	0012/0013	1.4/1.4	161 – 175

* Without part of the revolutions 102/103 when pointing to the Crab.

Table 2: PICsIT Energy Bands. Columns: (1) Channel number in standard mode; (2) Energy [keV].

Channels Standard (1)	Energy (2)	Channels Standard (1)	Energy (2)
	Single Events		Multiple Events
10 – 16	203 – 252	5 – 12	336 – 448
17 – 28	252 – 336	13 – 28	448 – 672
29 – 40	336 – 448	29 – 45	672 – 1036
41 – 56	448 – 672	45 – 74	1036 – 1848
57 – 82	672 – 1036	75 – 136	1848 – 3584
83 – 140	1036 – 1848	137 – 194	3584 – 6720
141 – 198	1848 – 3584	194 – 215	6720 – 9072
199 – 254	3584 – 6720	216 – 254	9072 – 13440

5 Cosmic–ray induced events

Since the beginning of the in–flight operations, it was clear that there were spurious events contaminating the detector in addition to the backgroud and source events([4]). The cause was identified in cosmic–ray induced events, that are roughly the 10% of the total events and affect mainly the energy bands below 300 keV (Segreto et al. 2003, see also Natalucci 2003). As underlined by Natalucci (2003) these fake events can significanly affect the performances of PICsIT. Moreover, there are also some noisy pixels (not hot pixels, that are killed by the onboard software), but it is not well known the origin of the noise (electronics?). Anyway, the effect on the detector of these problems is the same: to produce pixels with anomalous counts (see Fig. 3).

It is possible to perform a cleaning only in photon–by–photon mode, by acting on the single count. In standard mode, since only histograms are downloaded, an *a posteriori* correction is available: when the pixel counts are higher than a constant multiplied by the average count values, i.e. $counts > k \cdot average$, the pixel value is reset to the mean value. First tests showed a certain effectiveness of this correction, although the random nature of this type of correction introduces strong fluctuations in the count rates and significances in the reconstructed sky images.

This hypothesis is confirmed by the analysis of photon–by–photon data: indeed, in this case, it was possible to develop an algorithm to delete from the photon list those events that can be identified as fake.

[4]See some nice animations by the IBIS Team in Tübingen at http://astro.uni–tuebingen.de/groups/integral/anim_gif/.

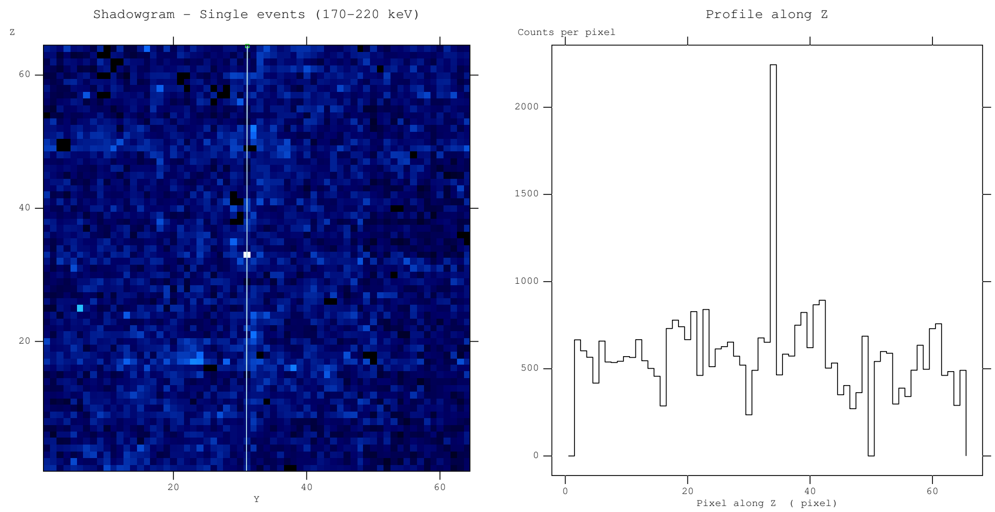

Figure 3: Effect of cosmic-rays induced events and/or noisy pixels on the shadowgrams. The white pixels have an anomalous high count value. This example is taken from the data of revolution 24 in the energy band 170 – 220 keV; PICsIT was in photon–by–photon mode.

File Edit Tools

	DELTA_TIME 1B	PICSIT_PHA 1I	PICSIT_Y 1B	PICSIT_Z 1B
1	123	30	45	22
2	128	25	54	62
3	130	35	36	4
4	132	30	15	9
5	133	39	11	56
6	139	40	62	33
7	141	39	31	57
8	146	24	13	18
9	150	24	13	18
10	152	24	13	18
11	154	25	13	18
12	156	24	13	18
13	157	28	31	20
14	159	24	13	18
15	163	24	13	18
16	164	24	13	18
17	166	24	13	18
18	167	73	42	48
19	167	26	2	24
20	176	28	19	3

Figure 4: Identification in the photon list (single events) of fake events produced by cosmic–rays and/or noisy pixels. Spurious events are emphasized in blue.

After having isolated some of these “tracks”, the photon list displayed series of photons “packed” in a very short time scale hitting a single pixel. Such “packets” are shown in Fig. 4, where fake events are emphasized in blue.

By removing these “packets” it is possible to obtain a cleaned shadowgram (Fig. 5), but – obviously – this is possible only when PICsIT is set to operate in photon–by–photon mode. Since the available telemetry is not sufficient for this type of mode, PICsIT works almost always in standard mode (i.e. with events integrated onboard in histograms). In this mode, there is no possibility to act on the single photon and, therefore, it is possible only to operate the *a posteriori* correction described above.

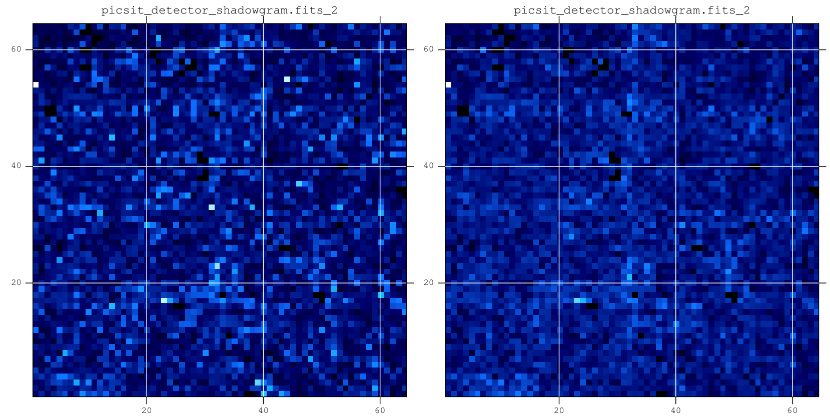

Figure 5: Effect of cosmic–rays induced events and/or noisy pixels on the shadowgrams (photon–by–photon mode). (*left*) Normal shadowgram; (*right*) Cleaned shadowgram. After the cleaning, the bright pixels disappeared. The only bright pixel remained at the top left of the cleaned shadowgram is a well–known pixel that often is hot. Data from revolution 14, energy band $170 - 250$ keV.

At the time of updating the present report, a study to remove these fake events onboard has been presented (Labanti et al. 2005). In this case, the cleaning would be performed on board before to integrate the histogram, so that the downloaded histogram would be cleaned from the cosmic-rays induced events. A set of observations of the Crab and an empty field in photon-by-photon mode have been performed in March 2005 (Rev. 300), to test the effectiveness of the proposed solution. Preliminary results show an increase of sensitivity below 250 keV by a factor of ~ 2, as expected. A more detailed study is ongoing.

6 The sky image reconstruction

Here are shown some performances of the PICsIT ISSW. Details on the techniques of the deconvolution are available in Goldwurm et al. (2003).

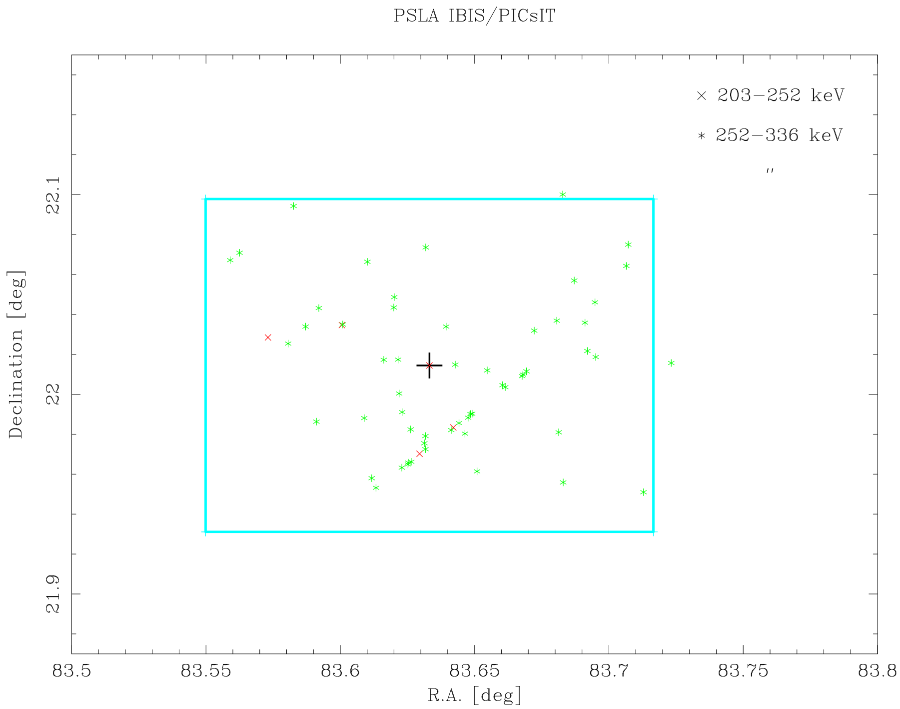

Figure 6: Sky coordinate reconstruction of the Crab position obtained with the ScW detections with $SNR > 3\sigma$ (Exposure 5 ks) in the energy band $252 - 336$ keV (*) and $203 - 252$ keV ($\times$). The catalog position of the Crab is shown at the centre of the figure and indicated with +. The surrounding square represents the pixel of PICsIT with $10'$ size.

6.1 Sky coordinates reconstruction

The sensitivity of PICsIT does not allow to see sources during a typical exposure of one ScW (2 ks), but there are sometimes Scw with duration of 5 ks. In this case, there is the possibility to detect the Crab at level of $SNR = 3 - 4\sigma$. During the observations of calibration performed in February 2003, the Crab was pointed during the revolutions 39, 43, 44, and 45 (staring and dithering hexagonal and 5×5). The coordinates of the Crab detected at $SNR > 3\sigma$ are reported in the Fig. 6. All the positions are within an error of $\pm 5'$ from the catalog position.

6.2 Image analysis

For the analysis of the Crab and the extraction of the reference count rates, we analyzed all the calibration observation performed from February 2003 to May 2005 (namely, Rev. $39 - 45$, 170, 239, 300, 365, 422) for an effective global exposure of 1.1 Ms.

The best performances of PICsIT are obtained with long background maps in the energy band $252 - 336$ keV, that is less affected by the cosmic–rays induced events and is in a range sufficiently low to detect enough photons.

Table 3: PICsIT observations of the Crab with OSA6. See the text for detailed explanations.

Energy Band (keV)	Rate Single Evts (c/s)	Rate Multiple Evts (c/s)
$203 - 252$	2.71 ± 0.02	–
$252 - 336$	2.46 ± 0.01	–
$336 - 448$	1.17 ± 0.01	0.07 ± 0.01
$448 - 672$	0.60 ± 0.01	0.14 ± 0.01
$672 - 1036$	0.26 ± 0.01	0.14 ± 0.01
$1036 - 1848$	0.06 ± 0.01	0.12 ± 0.01

The greatest differences in the count rates and significance (for observations in staring, dithering, off axis) occur just the band $203 - 252$ keV, where we expect that the impact of cosmic–ray induced events is still high and the *a posteriori* correction – the only available since PICsIT is operated in histogram mode – may not be too much accurate (see Sect. 5).

It is worth mentioning that during the observations of the calibration sources some tests of the photon-by-photon mode have been set up and performed, with special telemetry allocation to PICsIT (e.g. revolutions 39 and 40). However, despite this configuration, the limited telemetry budget resulted in a loss of about 80% of the pointing time. From an observation 100 ks long at the beginning of the revolution 40, the effective exposure is only 23 ks. An inspection of the GTI table and of the lightcurve revealed that the missing time was due to telemetry gaps.

7 Spectra

In OSA 6 a new set of RMF/ARF for PICsIT has been released. It includes an updated version of the response for single events and the first working response for multiple events.

Two ways are presently available to extract single sources spectra from PICsIT data: the first, and also the more reliable and stable, uses the count rates and errors obtained from the imaging pipeline. That is, OSA for PICsIT is run up to IMA2 level, then the mosaic is done, and the detected source count rate and error are read from the intensity and significance maps. M. Chernyakova (ISDC) has also prepared a Perl script to make these operations automatic[5].

An example of the Crab spectrum as seen by the whole IBIS instrument is shown in Fig. 7. The IBIS/PICsIT spectra (single and multiple events) have been extracted from the images obtained from the data set described in the Sect. 6.2. A systematic error of 5% was added to the first energy bin ($203 - 252$ keV), since it is mostly affected by cosmic-rays induced events.

ISGRI data have been extracted from rev. 102 by using OSA 5.1 and a systematic error of 1% was added.

The resulting spectrum fitted in the energy band 20 keV – 10 MeV with the usual power-law model gave $\Gamma = 2.11^{+0.09}_{-0.08}$ and normalization at 1 keV equal to $8.1^{+4.9}_{-2.8}$ ph cm^{-2} s^{-1} keV^{-1}, with intercalibration constants between ISGRI (set as reference) and PICsIT (single events) equal to $0.52^{+0.04}_{-0.03}$ and to 0.31 ± 0.06 for multiple events. Despite the low values of the intercalibration constants, the photon index and normalization are consistent with the usual "standard" values given by the classic paper by Toor & Seward (1974), specifically $\Gamma = 2.10 \pm 0.03$ and $N = 9.7 \pm 1.0$ ph cm^{-2} s^{-1} keV^{-1}. A more recent study by Kirsch et al. (2005), after the analysis of several high-energy satellites in the energy band $0.1 - 1000$ keV, gave a the values of $\Gamma = 2.08$ and $N = 8.97$ ph cm^{-2} s^{-1} keV^{-1}, still consistent with the

[5] The script is publicly available at `http://isdc.unige.ch/index.cgi?Soft+scripts`.

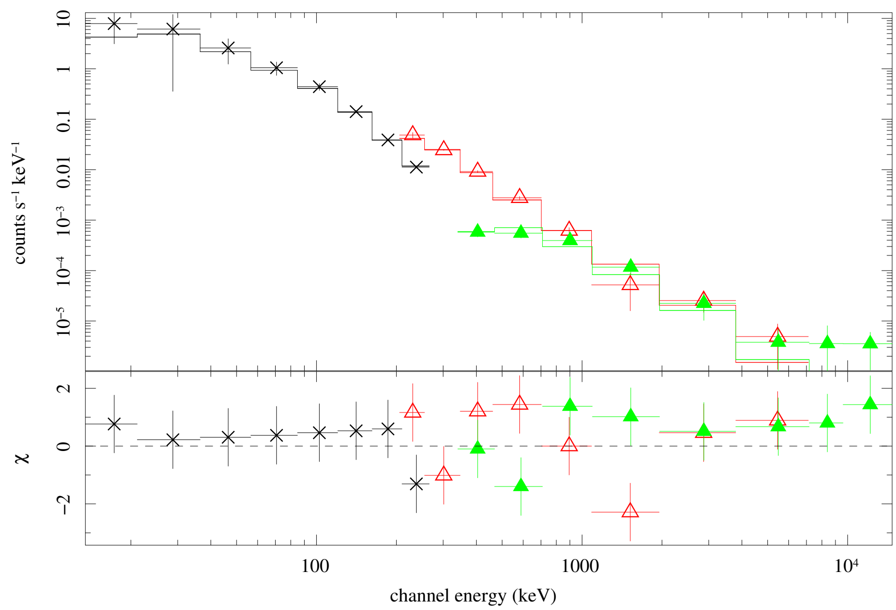

Figure 7: IBIS (ISGRI+PICsIT) spectrum of the Crab. Data of ISGRI are indicated with $\times$, while open triangles are for PICsIT single events and filled triangles for PICsIT multiple events.

results obtained with OSA 6 for IBIS/PICsIT.

The other way is to run the pipeline from BIN_S to SPE level, thus using the `ip_spectra_extraction` module. However, since PICsIT sources are very faint in a high background[6] and results are not yet satisfactory. An alternative solution is currently under study.

Presently, it is better to use the first way (imaging) – although limited by the availability of background maps – that gives the best reliable results. A clear example is presented in Cadolle-Bel et al. (2005), where the spectrum of Cyg X-1 is presented, together with the other instruments. Another example is shown in Bianchin et al. (2006), with the analysis of XTE $J1550-564$.

8 Timing

When set in standard mode, PICsIT generates also spectral timing data in addition to imaging histograms. These data are useful to build lightcurves with high timing performances ($\approx 1-500$ ms time resolution).

Starting from Rev. 441 the spectral timing mode has been set to this new values: 8 energy bands ($208-260$, $260-312$, $312-364$, $364-468$, $468-572$, $572-780$, $780-1196$, $1196-2600$ keV) with 16 ms of time resolution, in order to explore the MeV energy range. This could be useful particularly in studies of GRB, coordinated with Compton mode, since PICsIT is the only instrument presently available, able to reach the MeV energy range. A new set of RMF/ARF is currently under evaluation and preliminary results are available in Di Cocco et al. (2007). It is foreseen to release these new responses in the future version of OSA.

[6]It is worth reminding that the Crab has a count rate of less than 10 c/s over the whole energy range for single events, to be compared with a background of about 2500 c/s.

9 Known problems in OSA for PICsIT and things to do

Presently, these were the problem known in the OSA 6 for PICsIT:

1. The spectra extraction with PIF method (executable `ip_spectra_extraction`) is not reliable for the moment. The user should extract the spectra from images (count rates from intensity maps and errors from significance maps) and then convolve them with the RMF/ARF.
2. The value of `FLUX_ERR` column in the file `pics_sky_res.fits` is not correct. The error can be calculated from the `DETSIG` column (SPR 4642).
3. In the first energy band ($203 - 252$ keV), when PICsIT cannot find any evident source, the software catches the first source in the catalog (SPR 4638). Obviously this has no physical meaning.
4. Phase shift in spectral timing mode.

Major improvements to be added in OSA for PICsIT are: mask transparency, PIF calculation for off-axis sources, improvement of background subtraction for very long mosaics, full use of multiple events.

10 Final remarks

Further informations, presentations, reports on PICsIT, together with the catalog of the sources detected to date, are available at the IBIS/PICsIT web page at INAF/IASF-Bologna, created and maintained by F. Schiavone:

`http://www.iasf-bologna.inaf.it/Research/INTEGRAL/`

Hints and tricks in PICsIT data analysis can be found in:

`http://www.iasf-bologna.inaf.it/~foschini/OSAP/picsit_data_analysis.html`

11 References

- Bianchin V., Foschini L., Sambruna R.M., et al., 2006, Proceedings of the VI Microquasar Workshop, PoS(MQW6)072 (http://pos.sissa.it//archive/conferences/033/072/MQW6_072.pdf)
- Cadolle Bel M., Sizun P., Goldwurm A., et al., 2005, A&A 446, 591.
- Calabretta M.R., Greisen E.W., 2002, A&A 395, 1077
- Di Cocco G., Caroli E., Celesti E., et al., 2003, A&A 411, L189
- Di Cocco G., Bianchin V., Foschini L., et al., 2007, Proceedings of the VI INTEGRAL Workshop, to be published.
- Ebisawa K., Bourban G., Bodaghee A., et al., 2003, A&A 411, L59
- Ferguson C., Barlow E.J., Bird A.J., et al., 2003, A&A 411, L19
- Kirsch M.G.F., Briel U., Burrows D., et al., 2005, Proceedings of the SPIE 5898, 22 (astro-ph/0508235)
- Goldwurm A., Goldoni P., Gros A., et al., 2001, In: "Exploring the gamma–ray universe. Proceedings of the Fourth INTEGRAL Workshop", 4-8 September 2000, Alicante, Spain. Editor: B. Battrick, Scientific editors: A. Gimenez, V. Reglero, and C. Winkler. ESA SP–459, p. 497.
- Goldwurm A., David P., Foschini L., et al., 2003, A&A 411, L223
- Labanti C., Di Cocco G., Marisaldi M., et al., "Proposal for recovering PICsIT low energy range", March 2005.
- Laurent P., Limousin O., Cadolle Bel M., et al., 2003, A&A 411, L185
- Malaguti G., Bazzano A., Bird A.J., et al., 2003, A&A 411, L173
- Natalucci L., Bird A.J., Bazzano A., et al., 2003, A&A 411, L209
- Segreto A., Labanti C., Bazzano A., et al., 2003, A&A 411, L215
- Toor A., Seward F.D., 1974, AJ 79, 995